Table 1 Laboratory data on admission

Blood Cell Count: WBC 5850 (Stab 4.0, Seg 78.0, Lym 11.0, Mono 7.0), RBC 429¥ 10^4, Hb 14.4 g/dL, Plt 11.0¥ 10^4
Coagulation Tests: PT 9.8% (INR 6.88), Fibrinogen 87 mg/dL, FDP 9.3 mg/mL
Biochemistry: Na/K/Cl 133/3.8/99 mM, TP 5.7 g/dL, Alb 3.2 g/dL
BUN 7.5 mg/dL, s-Cre 0.6 mg/dL
AST 910 U/l, ALT 1752 U/l, LDH 511 U/l,
ALP 708 U/l, -GTP 150 U/L, ChE 170 U/L
T-Bil 18.1 mg/dL, D-Bil 7.7 mg/dL (D/T = 0.425)
CRP 0.7 mg/dL, NH_3 212 mg/dL
Viral Markers: HBsAg (+) (EIA titer 184.83)
IgM-HBc Ab (-), HBc Ab/CLIA (+)
HBeAg (-), HBeAb (+) (99.8% inhibition)
HBV-DNA/TMA 6.6 LGE/mL, HDV-DNA (-)
HCV-Ab (-), IgM-HA-Ab (-), HEV-DNA (-)
CMV-Ab IgG 10>, CMV-IgM 10>
EBV-anti VCA IgG¥ 80?IgM 10>
Others: ANA 20.2, anti DNA antibody 80, Anti Mitochondria Ab 20>

findings were noted at annual physical check-up. He was considered to be an asymptomatic HBV carrier. The patient was hospitalized on the day of his first visit. Follow-up tests showed worsening of liver enzyme levels and an alteration in consciousness level was noticed after 2 days. The patient was then referred to Tsukuba Gakuen Hospital as the development of acute liver failure was of concern.

Laboratory data on arrival are shown in Table 1. Elevation of serum ALT (1754 IU/L) and hyperbilirubinemia (T-Bil, 18.1 mg/dL) were observed. The patient was positive for HBVs antigen and HBe antibody, but markers for other types of viral hepatitis, including hepatitis A virus, hepatitis C virus, hepatitis D virus and hepatitis E virus were all negative. The HBV-DNA level was found to be more than 6.6 log genome equivalents (LGE)/mL using transcription-mediated amplification. Prothrombin time was markedly prolonged (PT% = 20) and an atrophic liver was apparent on abdominal ultrasonography. The patient showed disorientation and pronounced confusion on the day of arrival, and thus was diagnosed with grade III hepatic encephalopathy. He was immediately placed on artificial liver support (ALS) comprising plasma exchange and hemodiafiltration[2] with a combination of interferon beta and lamivudine, only nucleic acid analog approved by Japanese National health Insurance system at this time, as antiviral therapy (Fig. 1). A large dose of methylpredonisolone was also administered to suppress a presumably enhanced host immune response.[3]

In parallel, we started to discuss liver transplantation with his family. The patient had four brothers, and three were considered as possible donors for orthopedic liver transplantation. However, screening by blood tests and ultrasonography showed that the three brothers were positive for HBs antigen, and therefore all were excluded as donor candidates. A cadaveric liver was unavailable and thus we had to give up on liver transplantation. Despite intensive care, the patient complicated with acute respiratory distress syndrome (ARDS) and acute renal failure, and died on the 8th day of admission.

GENETIC ANALYSIS OF HBV

WITH THE PERMISSION of the family members, genetic analysis of HBV in serum acquired from the patient and family members was performed. HBV DNA sequences spanning the S gene were determined by real-time PCR according to the method of Abe *et al.*,[4] with a detection limit of 100 copies/mL. HBV DNA sequences bearing the CP, PC region, and core gene were amplified by PCR using hemi-nested primers, as described previously.[4] The neighbor-joining method[5] was used for phylogenetic analysis of the S region to classify HBV into subgenotypes. To confirm the reliability of the phylogenetic tree, bootstrap re-sampling tests were performed 1000 times.

Only the third sibling ("sibling C" in Table 2) showed an elevated ALT level (50 IU/L), with ALT levels in the

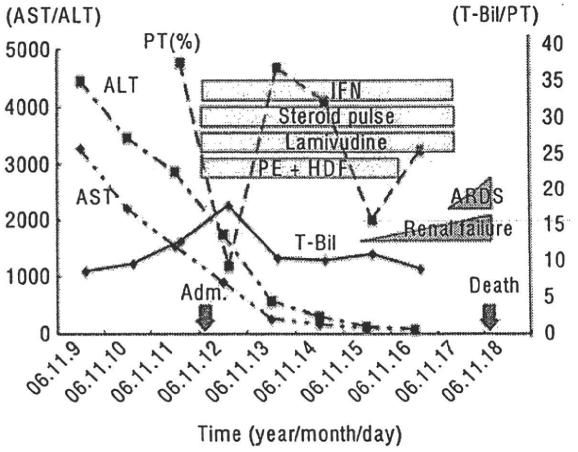

Figure 1 Clinical Course of the patient. ARDS, acute respiratory distress syndrome; HDF, hemodiafiltration; IFN, interferon beta; PE, plasma exchange; PT, prothrombin time.

Table 2 Profile of each sibling

	Age	Sex	AST/ALT	HBV-DNA	HBeAg	1896A/1899A/CP
Patient	41	M	910/1752	6.02 log copy/mL	–	+/+/+
Sibling A	45	M	36/35	5.25 log copy/mL	–	+/-/-
Sibling B	36	M	28/32	4.68 log copy/mL	–	+/-/-
Sibling C	31	M	31/50	<2.6 log copy/mL	–	+/+/-

other siblings within the normal range (about 40 IU/L). None of the siblings were HBeAg-positive. HBV-DNA loads were highest in the patient, relatively lower in sibling A and B, and under the detectable range in sibling C (Table 2). The HBV genotype was determined based on analysis of the S region. All siblings were infected with HBV-Bj, a subgenotype that is predominantly detected in patients who reside in a specific geographical location (including Okinawa prefecture) in Japan. HBV-DNA of patient and all siblings formed same cluster, thus it is speculated that they were infected from same source. In fact, the presence of family history of hepatic disease (their mother died by it) strongly suggests the vertical infection (Fig. 2). Mutations in the PC (G1896A) and CP (A1762T/G1764A) were also discovered. As shown in Figure 3, the patient and all siblings had the 1896A mutation, which is consistent with the absence of HBeAg, and the patient had both the G1899A and CP mutations (A1762T/G1764A). Sibling C had the G1899A mutation but not the CP mutation, and the other siblings had none of these mutations.

DISCUSSION

FULMINANT VIRAL HEPATITIS is thought to occur as a result of immunoreactions against enhanced viral replication. Findings associated with immunoresponses of hosts in fulminant cases are limited, probably due to the absence of definitive methodology for determination of individual immunoresponses. However, factors associated with viral replication have been investigated, and an HBV subgenotype and PC and CP mutations have been linked to high replication rates in acute HBV infection and in turn to fulminant outcome.[1] Besides fulminant hepatitis caused by acute infection of HBV, fatal acute liver failure may also emerge from a previously unrecognized chronic infection of HBV, but little is known about the viral factors involved in acute exacerbation in chronic HBV carriers.

In the current case, the patient was infected with the HBV/Bj subgenotype, was HBeAb-positive, and had PC and CP mutations. Although the patient was already an HBV carrier at the time of onset, his genomic profiles matched the pattern frequently seen in fulminant hepatitis caused by acute HBV infection.[1] Among the population of HBV carriers, patients infected with HBV/Ce and HBV/Bj are predominant in Japan.[6–9] HBV/Bj is a specific subgenotype that is present in less than 10% of HBV carriers, but has a higher prevalence in locations such as the Northeastern (Tohoku) district of Honshu and in Okinawa. Patients with HBV/C infection tend to have chronic sustained inflammation that progresses to liver cirrhosis and hepatocellular carcinoma, whereas HBV/Bj more frequently induces HBe seroconversion via a PC mutation, which results in a lower viral load and reduced disease severity.[10]

Sugiyama *et al.* determined the intracellular and extracellular HBV DNA levels in Huh-7 cells transfected with a plasmid carrying different genotypes/subgenotypes of the HBV genome without a CP/PC mutation.[11] HBV DNA levels in cell lysates were highest for HBV/C, followed by Bj/Ba and D/Ae, and lowest for Aa; whereas in culture media these levels were highest for Bj, with much lower levels for Ba/C/D, and still lower levels for Ae/Aa.[11] It was speculated that the strong tendency of Bj for extracellular virion secretion may endow a high infectious capacity to blood from individuals infected with this subgenotype, and that this may trigger strong immune responses in hosts.[11] This characteristic of HBV/Bj is thought to be associated with earlier seroconversion from hepatitis Be antigen (HBeAg) to the corresponding antibody (anti-HBe) and with lower histological activity.

Acute exacerbation of chronic liver disease (CLD) has been seen in some patients with chronic HBV/Bj infection post-seroconversion, with a fatal outcome similar to that in the current case. In a study of 592 patients, no significant difference in the frequency of genotype B was found between patients with CLD and those with acute exacerbation of CLD (62/531 [11.7%] versus 4/19 [21.1%]; NS),[12] but acute exacerbation was seen more frequently in CLD patients with HBV/B infection (4/62, 6.5%) compared to those with HBV/C infection (13/459, 2.8%).[12] The PC stop codon mutation (G1896A)

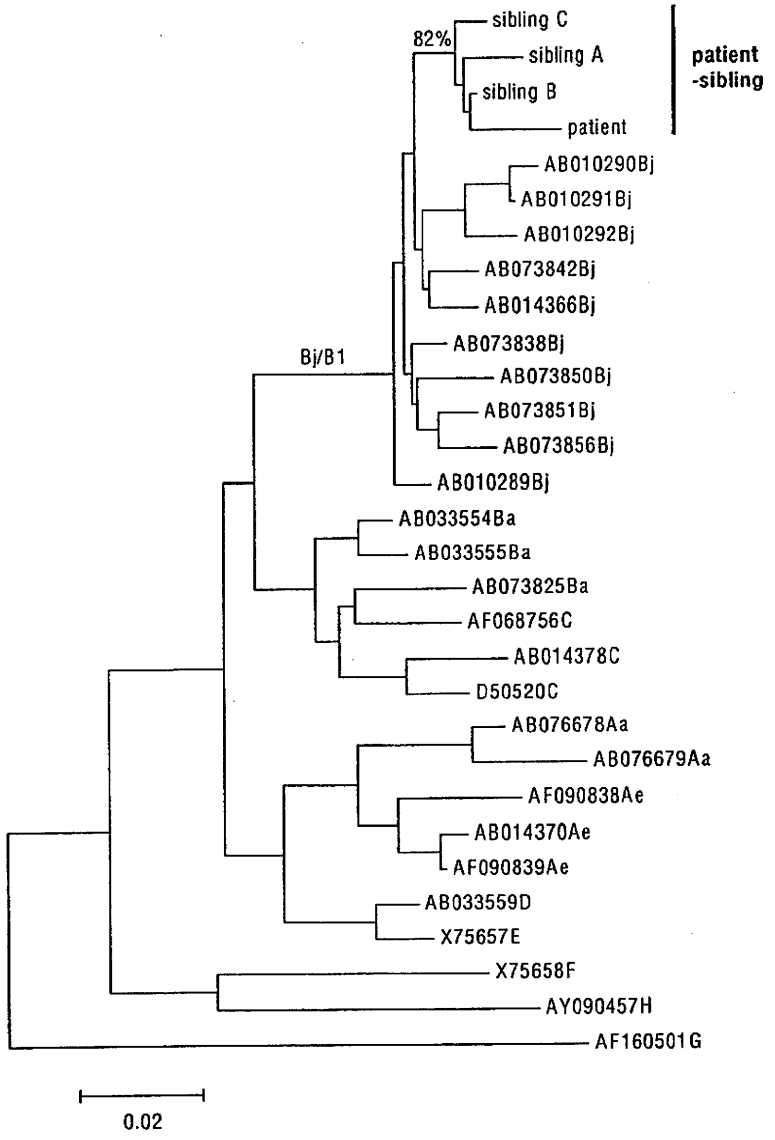

Figure 2 Subgenotyping of hepatitis B virus (HBV). HBV subgenotype was determined by sequencing of the S gene. Result of phylogenetic analysis of sequences from the pre-S region of HBV in the patient and siblings and reference strains from a database was shown. Reference strains were shown by accession number. The scale bar indicates genetic distance.

and the CP double mutation (A1762T/G1764A) were detected more frequently in HBV/Bj-infected patients with fulminant hepatitis compared to those with acute-self limited hepatitis (56% vs. 0%, and 67% vs. 0%).[1] These findings suggest that the replication potential of HBV/Bj might be stronger in the presence of CP/PC mutations than in the wild type virus, and Ozasa *et al.* demonstrated enhanced replication capacity of HBV/Bj with PC or CP mutations compared to wild type *in vitro*.[1]

Although HBV/Bj may show highly potent replication, this may not be the cause of enhanced immunoresponsiveness in patients with chronic infection of HBV/Bj. Rather, CP/PC mutation in HBV/Bj post-seroconversion may be the factor that facilitates potent viral replication and acute exacerbation of CLD. The host-associated factor that influences outcome in patients with chronic HBV/Bj infection has not been identified, but these viral characteristics may be predictive factors for future exacerbation. In the current study, the patient had both PC (G1896A/G1899A) and CP mutations and a G1896A/G1899A mutation was found in one sibling. Although HBV-DNA load in this sibling is under detectable range right now, a CP mutation in the future on this sibling may lead to a fatal outcome.

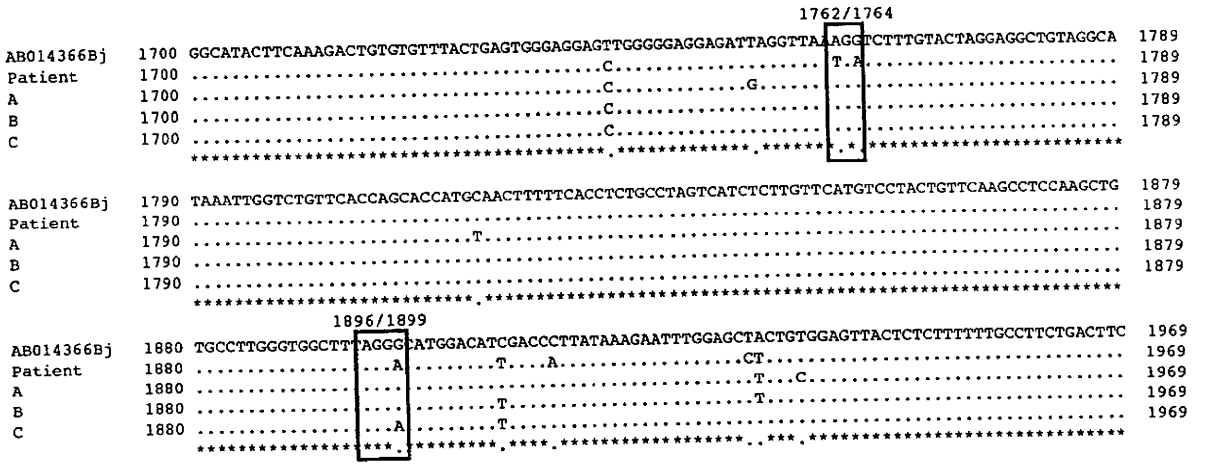

Figure 3 Nucleotide sequence of the core promoter/pre core region. Core promoter and pre-core region of hepatitis B virus (HBV) in the patient and siblings were determined. Mutation in core promoter (A1762T, G1764A) and precore (G1896A, G1899A) are indicated in boxes. The sequence of the reference HBV/Bj (AB014366Bj) is shown at the top of the figure.

Therefore, this sibling requires intensive follow-up and possible early administration of anti-viral drugs especially under the condition with immunosuppression, which can facilitate viral replication.

In conclusion, we suggest that analysis of the HBV subgenotype and CP/PC mutations should be performed during observation of asymptomatic HBV carriers to provide a more accurate understanding of the clinical presentation and to build an appropriate treatment strategy.

REFERENCES

1 Ozasa A, Tanaka Y, Orito E *et al.* Influence of genotypes and precore mutations on fulminant or chronic outcome of acute hepatitis B virus infection. *Hepatology* 2006; 44: 326–34.
2 Yoshiba M, Inoue K, Sekiyama K, Koh I. Favorable effect of new artificial liver support on survival of patients with fulminant hepatic failure. *Artif Organs* 1996; 20: 1169–72.
3 Masuhara M, Yagawa T, Aoyagi M *et al.* HBV-related fulminant hepatic failure: successful intensive medical therapy in a candidate for liver transplantation. *J Gastroenterol* 2001; 36: 350–3.
4 Abe A, Inoue K, Tanaka T *et al.* Quantitation of hepatitis B virus genomic DNA by real-time detection PCR. *J Clin Microbiol* 1999; 37: 2899–903.
5 Saitou N, Nei M. The neighbor-joining method: a new method for reconstructing phylogenetic trees. *Mol Biol Evol* 1987; 4: 406–25.
6 Sugauchi F, Orito E, Ichida T *et al.* Epidemiologic and virologic characteristics of hepatitis B virus genotype B having the recombination with genotype C. *Gastroenterology* 2003; 124: 925–32.
7 Tanaka Y, Orito E, Yuen MF *et al.* Two subtypes (subgenotypes) of hepatitis B virus genotype C: a novel subtyping assay based on restriction fragment length polymorphism. *Hepatol Res* 2005; 33: 216–24.
8 Takeda Y, Katano Y, Hayashi K *et al.* Difference of HBV genotype distribution between acute hepatitis and chronic hepatitis in Japan. *Infection* 2006; 34: 201–7.
9 Hayashi K, Katano Y, Takeda Y *et al.* Comparison of hepatitis B virus subgenotypes in patients with acute and chronic hepatitis B and absence of lamivudine-resistant strains in acute hepatitis B in Japan. *J Med Virol* 2007; 79: 366–73.
10 Hagiwara S, Kudo M, Minami Y *et al.* Clinical significance of the genotype and core promoter/pre-core mutations in hepatitis B virus carriers. *Intervirology* 2006; 49: 200–6.
11 Sugiyama M, Tanaka Y, Kato T *et al.* Influence of hepatitis B virus genotypes on the intra- and extracellular expression of viral DNA and antigens. *Hepatology* 2006; 44: 915–24.
12 Imamura T, Yokosuka O, Kurihara T *et al.* Distribution of hepatitis B viral genotypes and mutations in the core promoter and precore regions in acute forms of liver disease in patients from Chiba, Japan. *Gut* 2003; 52: 1630–7.

Hepatology Research 2009; 39: 585–594 doi: 10.1111/j.1872-034X.2009.00495.x

Original Article

Regulatory T cells and liver pathology in a murine graft versus host response model

Teruo Miyazaki,[1,2] Mikio Doy,[3] Tadashi Ikegami,[4] Akira Honda,[1,2] Rie Unno,[5] Shinichi Itoh,[4] Bernard Bouscarel[6] and Yasushi Matsuzaki[1,4]

[1]Department of Development for Community Medicine, Tokyo Medical University, [2]Center for Collaborative Research, Tokyo Medical University Ibaraki Medical Center, [4]Department of Internal Medicine, Division of Gastroenterology and Hepatology, Tokyo Medical University Ibaraki Medical Center, Ami, [3]Ibaraki Prefectural Central Hospital, Kasama, [5]Unno Clinic, Moriya, Japan; and [6]Department of Biochemistry and Molecular Biology, The George Washington University, District of Columbia, USA

Aim: We have previously reported in mice the hepatic inflammatory in graft versus host response (GVHR) model due to the disparity of major histocompatibility complex class-II. The regulatory T (Treg) cells have been reported to control excessive immune response and prevent immune-related diseases. This study aimed to investigate the pathogenesis profiles of chronic GVHR progression, focusing on the Treg cells.

Methods: GVHR mice induced by parental spleen CD4$^+$ T cell injection were sacrificed after 0, 2, 4, and 8 weeks (G0, G2, G4, G8). Further, one GVHR group received anti-IL-10 antibody in advance and were maintained for 2 weeks. Pathologic profiles of hepatic infiltrating inflammatory cells were evaluated by haematoxylin and eosin and immunohistochemistry staining with surface markers including Treg cell markers.

Results: Remarkable hepatic inflammatory in G2 significantly and gradually improved over time up to G8. In immunohistochemical staining, the increased IL-10 receptor β^+ Tr1 cells in G2 were maintained through to G8; although other inflammatory cells decreased from G2 to G8. By contrast, in the anti-IL-10 antibody received-GVHR mice, the Tr1 cells were not detectable with significant inflammatory aggravation, while FoxP3$^+$ Treg cells significantly enhanced.

Conclusions: These findings in the GVHR mice suggest that the expression and activity of Treg cells, especially the Tr1 cells, might be key factors for pathologic alteration in immune-related liver disease.

Key words: Graft versus host response disease, Immunohistochemistry staining, Regulatory T cells, Tr1 cells

INTRODUCTION

WE HAVE PREVIOUSLY reported that the injection of parental CD4$^+$ T cells into F1 hybrid mice induced graft versus host response (GVHR) hepatitis due to the disparity of the major histocompatibility complex (MHC) class II.[1–5] The GVHR mice have histological and immunological alterations similar to those observed in primary biliary cirrhosis (i.e. infiltration of lymphocytes in the periportal region, pericholangitis around the interlobular bile duct, and the presence of anti-mitochondrial antibodies of a recipient origin).[6] In the histological and immunological observations of the GVHR model over a period of 2 weeks, the inflammatory cells, including CD4$^+$T cells, CD8$^+$T cells, B cells, and macrophages, infiltrated into the hepatic tissue as early as 3 days after the parental T cell transfer, and the inflammation developed within 2 weeks. Differential profiles of inflammatory-related cytokines were observed in the hepatic tissues between Th1- and Th2-derived cytokines in a manner that was dependent on the GVHR progression during this period.[2] A significantly higher level of interferon (IFN)-γ mRNA was observed after 3 days and was maintained for at least 2 weeks. On the other hand, the interleukin (IL)-10 mRNA expression was not detectable at 3 days, but was significantly increased by the 2-week time point.

Notably, the GVHR model does not lead to liver cirrhosis, because the serum aminotransferases levels

Correspondence: Dr Yasushi Matsuzaki, Department of Internal Medicine, Division of Gastroenterology and Hepatology, Tokyo Medical University Ibaraki Medical Center, 3-20-1, Chuo, Ami, Ibaraki, Japan. 300-0395. Email: ymatsuzaki-gi@umin.ac.jp
Received 15 October 2008; revision 12 November 2008; accepted 26 December 2008.

remained unchanged throughout the study period and fibrosis did not appear after 2 weeks.[2–5] It has been considered that the GVHR would cause abrogation of immune-tolerance because the transferred parental T cells invade at the site of the hepatic lesions due to the differences in MHC class II.[7] The abrogation of self-tolerance has been known to cause autoimmune diseases,[8] and can be prevented by the regulatory T (Treg) cells, which are a subset of the $CD4^+$T cells.[9–11] The Treg cells play important roles in controlling excessive immune response and preventing immune-related diseases.[10] The Treg cells can be characterized into different subsets based on surface markers, cytokine profiles, and suppressing functions; $CD4^+CD25^+$Treg cells, IL-10 receptor $(R)^+$ type 1 Treg (Tr1) cells, and $CD4^+CD161^+$ natural killer T (NKT) cells.[10,12,13]

We hypothesized that the Treg cells might influence the progression of the liver pathology in the GVHR, because this model shows abrogation of immune-tolerance. In the present study, we investigated the pathogenesis profiles on the progression of chronic GVHR over a period of 8 weeks, focusing on the time-dependent relationship between the progression of the inflammatory lesions and the expression of the Treg cells in the hepatic tissue by histological analyses.

MATERIALS AND METHODS

GVHR animal model

C57BL/6(B6)[*H-2K*^{b}, *I-A*^{b}, *H-2D*^{b}] mice were purchased from the Charles River Japan (Atsugi, Japan). B6.*C-H-2*^{bm12}(bm12)[*H-2K*^{b}, *I-A*^{bm12}, *H-2D*^{b}] mice with mutation at the I-A region, originally from the Jackson Laboratory (Bar Harbor, ME, USA), were used to obtain (bm12 × B6) F1 hybrid mice. All animals received humane care in accordance with the guidelines of the University of Tsukuba for the care of laboratory animals.

Female F1 mice, between 10 and 15 weeks of age, received donor B6 T cells for the induction of GVHR as previously reported.[5,14] Briefly, sex-matched $1\sim2 \times 10^7$ B6 T cells were injected into recipients via the tail vein. Five recipient mice were sacrificed immediately, or 2, 4, and 8 weeks after the cell transfer (G0, G2, G4, G8). Furthermore, the anti-IL-10 monoclonal antibody (mAb)-injected GVHR model mice were induced according the method described in our previous study.[5] Either the IL-10 mAb (JESO52A55 Genzyme/Techne, Cambridge, MA, USA) or control mAb (Rat IgG1 Isotype Control, 43414.11 Genzyme/Techne) dissolved in pathogen-free saline were injected intraperitoneally at a dose of 500 mg per mouse 4 h before the cell transfer, and five mice per group were sacrificed at 2 weeks. Anaesthetized with pentobarbital, the liver was perfused with 2 mL PBS via the portal vein to washout the blood from the liver. Tissues including liver, spleen, lung, heart, kidneys, and bone marrow were embedded in paraffin after fixation in 10% formalin for histological studies including including Haematoxylin and eosin (H&E) and immunohistochemical (IHC) stains.

H&E stain

The H&E staining was conducted using a standard method. The H&E images were captured into a computer, and the areas of infiltration of inflammatory cells into the hepatic tissue were analyzed using Image J software (NIH, Bethesda, MA, USA). In addition, the numbers of total inflammatory cells in the lesion were counted.

IHC stain

IHC stain was carried out using the auto-stain Discovery-XT system with the proprietary reagents (Ventana, Tucson, AZ, USA). In the case of mouse monoclonal antibodies, the MoMap kit (Ventana) was used to avoid any reactions with non-specific antigens in mouse tissues. The mouse antibody was previously reacted with biotin-conjugated anti-mouse IgG antibody, and then, applied to the tissue slide after deactivation of any non-reacted IgG antibodies by reaction with mouse serum. The monoclonal antibodies used were as follows: CD4; CD8; CD20 (pre-diluted; Ventana), CD45ro (1:100; Chemicon International, Temecula, CA, USA), CD25; IL-2Rα (surface marker for $CD4^+CD25^+$Treg cells; pre-diluted; Lab vision, Fremont, CA, USA), X-linked forkhead/winged helix transcription factor (Foxp3; master gene of $CD4^+CD25^+$Treg cells; 1:100; Affinity Bioreagent, Golden, CO, USA).[12,15–18] The polyclonal antibodies were as follows; CD161 (1:100; Santa Cruz, CA, USA), IL-10Rβ (surface marker for the Tr1 cells; 1:100; Sigma, St. Louis, MO, USA). The slides were incubated with the primary antibody for one hour at 37°C, and then, incubated with the biotin-conjugated universal secondary antibody (Ventana) for 32 min at 37°C. The development was performed using the DAB map kit (Ventana), and nucleus and cytoplasm were stained using the hematoxylin counterstain (Ventana) and bluing reagent (Ventana).

In the IHC stain, the positive cells to the respective antibody were counted, and the ratio of the positive cells in the G2, G4, and G8 to total inflammatory cells in G2 were calculated.

Fluorescence double IHC stain

The CD25&CD4, IL-10Rβ&CD4, or CD161&CD4 double positive cells of the infiltrated inflammatory cells at G2 were examined by fluorescence IHC double stain and detected by a laser confocal microscopy (FV1000, Olympus, Tokyo, Japan). In the CD25&CD4 double stain, the CD4 antibody and FITC-conjugated anti-mouse antibody (1:500, Santa Cruz), and the CD25 antibody and Texas Red (TR)-conjugated anti-mouse IgG antibody (1:500, Santa Cruz) were reacted in a tube in advance using the MoMap kit, respectively, and then, the CD4-FITC and the CD25-TR antibodies were applied to tissue slide. Likewise, the IL-10Rβ&TR-conjugated anti-goat IgG antibodies (1:500, Santa Cruz) and the CD4&FITC-conjugated anti-mouse IgG antibodies, and the CD161&FITC-conjugated anti-goat IgG antibodies (1:500, Santa Cruz) and the CD4&TR-conjugated anti-goat IgG antibodies (1:500, Santa Cruz) were used for the IL-10Rβ&CD4 and the CD161&CD4 double IHC stains, respectively.

Statistical analysis

All data presented are the mean ± SD, and significant differences between two group and among the groups were determined by unpaired student's *t*-test and one-way ANOVA Fischer's PLSD post hoc test, respectively, using Stat View software (SAS Institute, Cary, NC).

RESULTS

Hepatic histological observation

FIGURE 1 SHOWS the hepatic histological observations from 0–8 weeks after T cells injection (G0, G2, G4, and G8) by H&E staining. Infiltration of inflammatory cells including mononuclear cells into the hepatic tissue were observed in the portal region of the hepatic lobule in G2 (Fig. 1b), consistent with our previous studies,[2-5] while these infiltrations were not observed in G0 (Fig. 1a). In the hepatic tissues, there were no other histological changes including necrosis, fatty change, and fibrosis in any of the GVHR mice, however, some cells that show the juvenile characters including enlarged form, strangely shaped nucleus, and faint colored cytoplasm were observed in the hepatic lesion through G2 to G8 (Fig. 1e). The infiltrations of inflammatory cells were gradually and significantly reduced over time and up to G8 (Fig. 1c–d, Fig. 2). The quantified area of infiltrated inflammatory cell was significantly decreased in G8 compared to that in G2 and G4 (Fig. 2). Similarly, the numbers of region with inflammatory cells per hepatic tissue area were significantly lower in G8 compared with G2 (Fig. 2). Under these conditions, there were no notable inflammatory regions or histological alterations in other tissues examined, including spleen, lung, heart, kidneys, and bone marrow between G0 and G2 to G8 groups (Data not shown).

IHC stain

In the hepatic regions of infiltrated inflammatory cells, all examined markers (CD4, CD8, CD20, CD25, CD45ro, CD161, Foxp3, IL-10Rβ) were detectable by IHC stain at G2 (Fig. 3). These surface markers were also detectable in G4 to G8 but not in G0 (data not shown). Certain of the surface markers including CD25, CD4, CD161 and IL-10Rβ were studied by immunofluorescence in the liver at G2 (Fig. 4). Colocalization between CD25&CD4, IL-10Rβ&CD4, CD161&CD4 were clearly detected and all positive cells expressing both CD25 and IL-10Rβ also expressed CD4, while not all the CD161 positive cells expressed CD4 (Fig. 4).

Figure 5 presents the ratio of the cells that were positive for the specific surface marker to the total infiltrated inflammatory cells at G2 to G8. With the exception of the cells expressing IL-10Rβ, which presented similar level of expression from G2 to G8, all the other cells showed a significantly decreased expression at G4 and G8 vs. G2. Among the other organs studied, all the surface markers in the spleen and only CD20 in the bone marrow were detectable through G2 to G8 (Data not shown).

Anti IL-10 antibody injected GVHR model

Pre-treatment of anti-IL-10 mAb with the GVHR mice significantly increased in the hepatic infiltration of inflammatory cells compared with that in the control IgG mAb-received GVHR mice (Fig. 6a,b). These findings are in agreement with our previous report.[5] However, in the IL-10-mAb-received GVHR mice, there was no detectable positive cell for IL-10Rβ in the infiltrated regions as measured by IHC staining (Fig. 6c). On the other hand, the expression level of Foxp3 was significantly enhanced by approximately 40% throughout the infiltrated region in the IL-10mAb-injected GVHR mice when compared to that in the control IgG

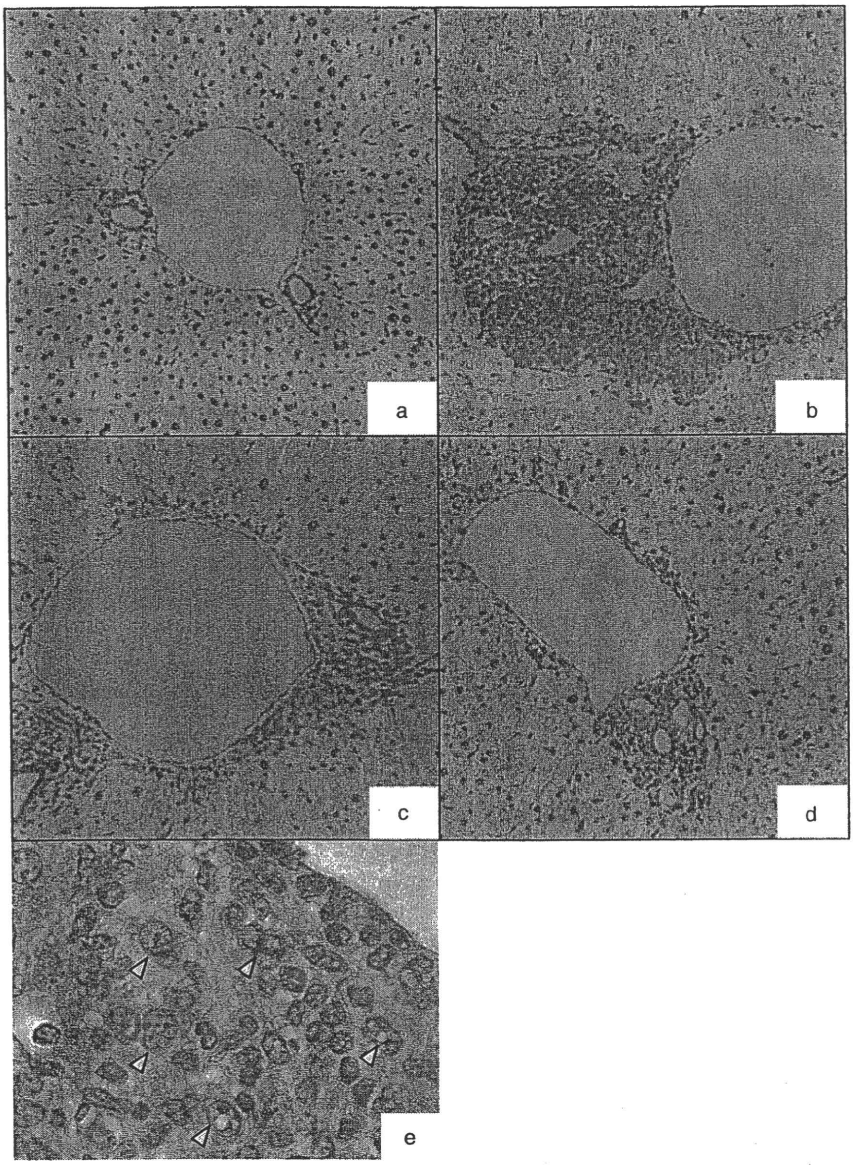

Figure 1 Hepatic histological observations of infiltrated inflammatory cells in the graft versus host response (GVHR) mice by haematoxylin and eosin stain. The triangle arrows in Fig. 1e show the cells with juvenile characters. (a) GVHR at 0 week (× 25). (b) GVHR at 2 weeks (× 25). (c) GVHR at 4 weeks (× 25). (d) GVHR at 8 weeks (× 25). (e) GVHR at 2 weeks (× 100).

mAb-receiving mice (Figs 6d,7). In the IHC stains, there were no differences in the profiles of infiltrated lymphocytes against all examined surface markers between the G2 mice without anti-IL10mAb and the control IgG mAb-injected mice.

DISCUSSION

THE PRESENT STUDY investigated the immune-related pathogenesis of hepatic inflammation throughout an 8-week period following injection of graft spleen T cells in the recipient mice. The hepatic infiltration of inflammatory cells reached a peak at

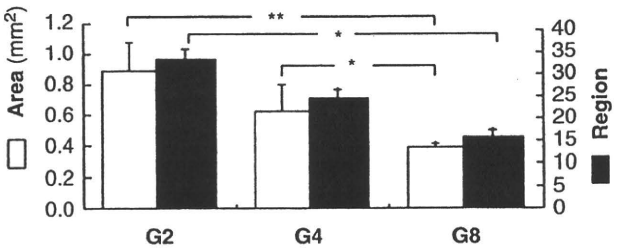

Figure 2 Area and number of regions with infiltrated inflammatory cells in the hepatic tissue. G2, graft versus host response (GVHR) mice at 2 weeks; G4, GVHR at 4 weeks; G8, GVHR at 8 weeks. Data are presented as the mean ± SD. $^{*}P < 0.05$; $^{**}P < 0.01$ by one way ANOVA Fischer's PLSD post hoc test.

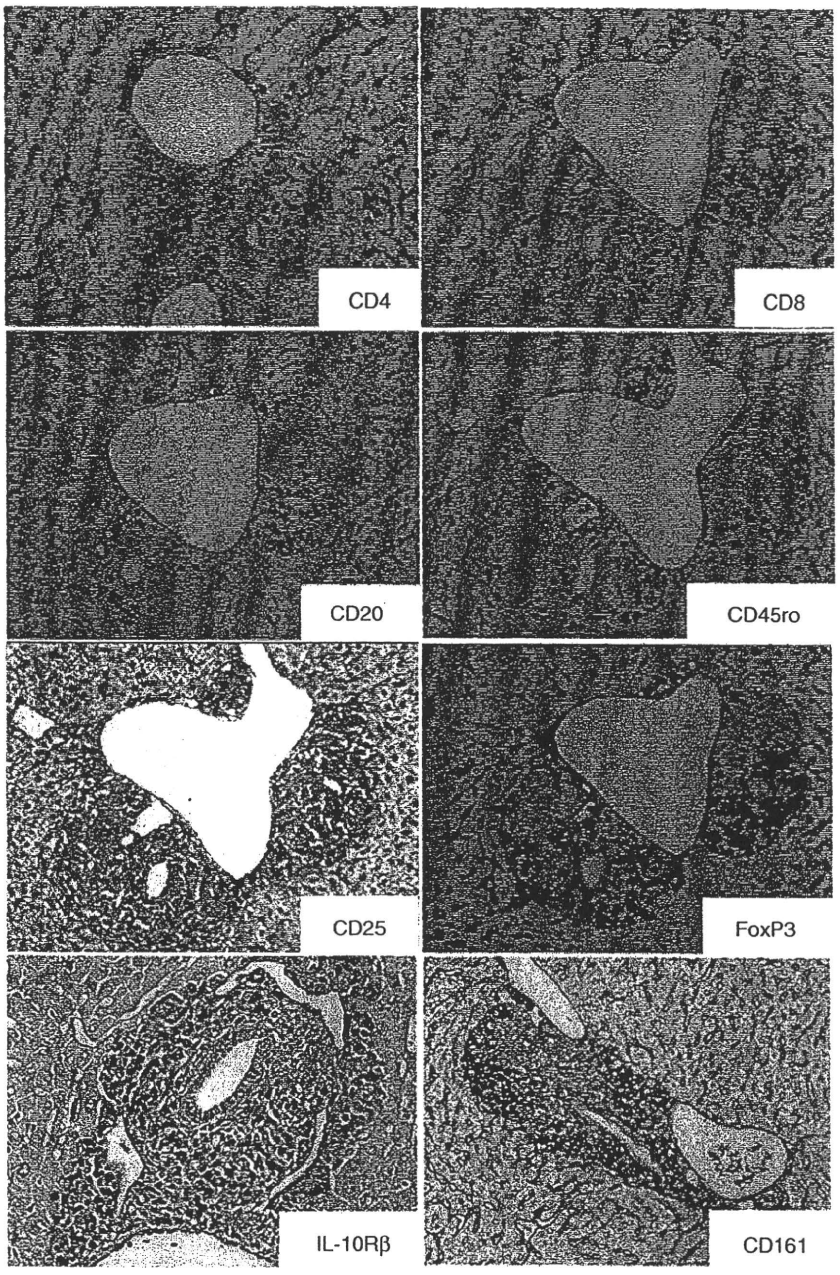

Figure 3 Hepatic immunohistochemical stained images of various surface markers of infiltrated inflammatory cells in G2 (×50).

2 weeks after the T cells transfer, as observed in our previous studies,[2–5] and gradually improved over the 8 weeks period studied. This progressive recovery from hepatic inflammation was a characteristic of the GVHR model mice, and clarifications of the mechanism(s) responsible for this recovery would have useful clinical impact for patients with immune-related liver diseases.

As preliminary experiment of this GVHR model, we analyzed comprehensive gene expressions of inflammatory-related cytokines in hepatic tissues infiltrated with inflammatory cells in G0, G2, and G8 by comparison of same age normal control without the T cells transfer using Panorama® Mouse Cytokine Gene array (Sigma). Among the genes that transiently increased at G2 and thereafter reduced at G8 along with the alteration of liver pathology, the highest expressed gene at G2 was IL-2Rγ that is one of three IL-2R subsets, α, β, and γ. The IL-2Rα is also named CD25 and is a

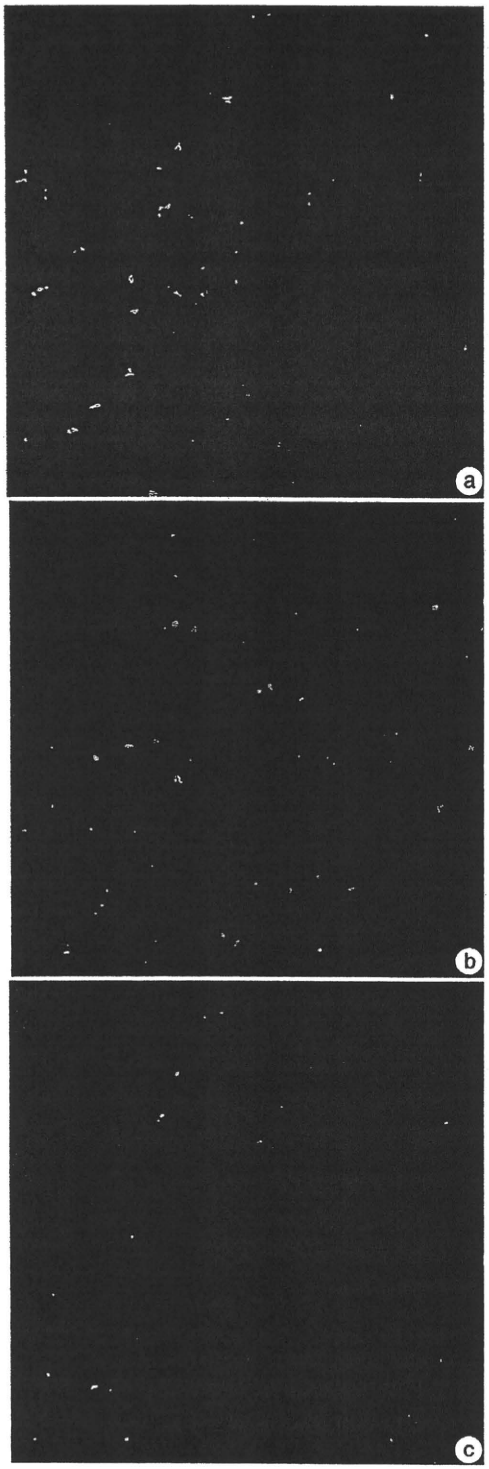

Figure 4 Merged fluorescence immunohistochemical observations of the surface markers for the regulatory T (Treg) cells in hepatic tissue of graft versus host response (GVHR) mice at 2 weeks. (a) $CD4^+$(FITC) $CD25^+$(TR) Treg cells. (b) $CD4^+$(FITC) $IL10R\beta^+$(TR) cells. (c) $CD4^+$(TR) $CD161^+$(FITC) cells. (× 60) TR, Texas Red.

specific surface marker of $CD4^+CD25^+$Treg cells, while the other two subsets are actual receptors for IL-2.[19] Based on these findings, we focused the present study on the influence of Treg cells including $CD4^+CD25^+$Treg cells, Tr1 cells, and NKT cells on the hepatic inflammation in the GVHR mouse model.

The Treg cells are subsets of $CD4^+$ T cells that are negative regulators in the immune responses. Among these cells, $CD4^+CD25^+$Treg cells and IL-10 producing Tr1 cells are the best-characterized Treg cells,[12] and NKT cells also behave as the Treg cells. The $CD4^+CD25^+$Treg cells were recognized by the co-expressing of CD4 and CD25 or the expression of master gene; FoxP3.[12] The Tr1 and NKT cells also have specific surface marker of IL-10R and CD161, respectively.[10,12,20]

Specific markers of Treg cells were detectable in the infiltrated inflammatory cells in the hepatic tissue from G2 to G8. These findings show the infiltration of the Treg cells into the inflammation region of the liver together with other lymphocytes. Furthermore, the ratio of the $IL\text{-}10R\beta^+$ cells (Tr1 cells) to the total infiltrated cells remained over the 8 weeks, while most of the other markers studied, including CD4, CD8, CD20, CD45ro, CD25, CD161, and FoxP3, were only transiently elevated with a significant reduction at 8 weeks along with the recovery in inflammation.

Previously, we have demonstrated that the injection of anti-IL-10 mAb into GVHR mice prior to that of the spleen T cells dramatically enhanced the hepatic infiltration of inflammatory cells after 2 weeks.[5] It has been previously reported that the IL-10 could decrease hepatotoxicity in several animal models[21–27] and ameliorate the inflammation of human HCV hepatitis.[28,29] Groux *et al.* have reported that the Tr1 cells with inflammatory properties produced high levels of IL-10.[30] In the present study, the expression level of the Tr1 cells was not detectable in the hepatic infiltration region of inflammatory cells in the anti-IL-10mAb injected GVHR mice, while this was detectable for up to 8 weeks in the GVHR mice that did not receive any anti-IL-10 mAb injection. This difference in the expression suggests that the anti-IL-10 mAb might be responsible for the loss of Tr1 cell expression in the hepatic inflammatory region, which would be compatible with the report that the Tr1 cells are activated by IL-10.[30,31] In the cDNA macroarray of the preliminary analysis, the gene expression levels of IL-10 and TGF-β elevated at G2 and maintained at G8 without anti-IL-10 mAb (data not shown). Interestingly, the expression of Foxp3, a master gene for the $CD4^+CD25^+$Treg cells, in the hepatic infiltration region was dramatically enhanced in the anti-IL-10mAb

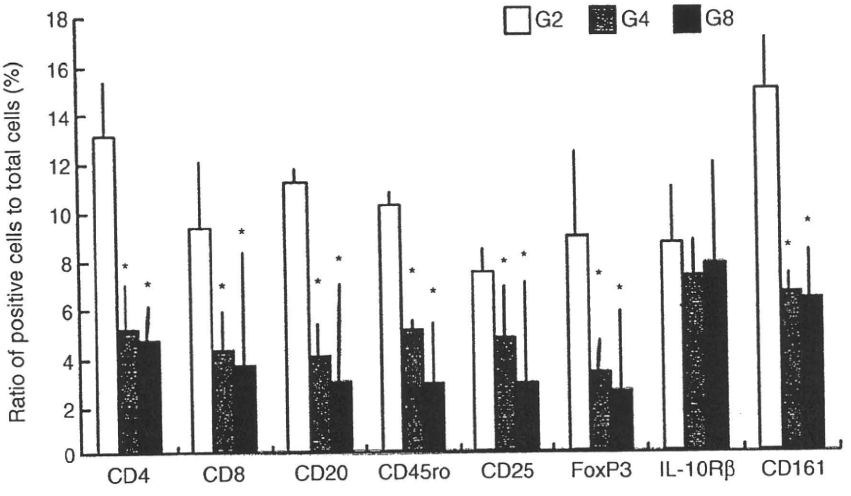

Figure 5 The ratio of the positive cells with the respective surface marker to the total infiltrated inflammatory cells in G2. The numbers of the positive cells and total cells were counted in the immunohistochemical and haematoxylin and eosin stained sections, respectively. G2, graft versus host response (GVHR) at 2 weeks; G4, GVHR at 4 weeks; G8, GVHR at 8 weeks. Data are presented as the mean ± SD. $*P < 0.05$ compared to G2 by one way ANOVA Fischer's PLSD post hoc test.

injected GVHR mice after 2 weeks assessed by IHC. The $CD4^+CD25^+$Treg cells and the Tr1 cells belong to the same subset of Treg cells at different stages of differentiation, and both Treg cells have an interactive relationship on their respective activations and functions.[10] The $CD4^+CD25^+$Treg cells typically differentiate in the thymus,[19] while the Tr1 cells differentiate in the periphery from native precursors, typically in the presences of IL-10 as well as TGF-β.[30,31] The $CD4^+CD25^+$Treg cells may contribute to the differentiation of the Tr1 cells by producing both IL-10 and TGF-β[32–34] and the activated Tr1 cells also produce IL-10 and TGF-β as autocrine factors.[31] In the observation on H&E stain, some undifferentiated and juvenile cells of lymphocytes were observed in the inflammatory region of hepatic tissue in the GVHR mice (Fig. 1e). Therefore, we hypothesized that the Tr1 cells were recruited as a native precursors into the hepatic lesion, and thereafter, were differentiated at the lesion influenced by the $CD4^+CD25^+$Treg cells. The immunologic reaction in the hepatic tissue receded after a transient inflammation at 2 weeks by expression of Treg cells, particularly in Tr1 cells. There is a possibility that the time lag between the transient inflammation and subsequent recovery might be due to

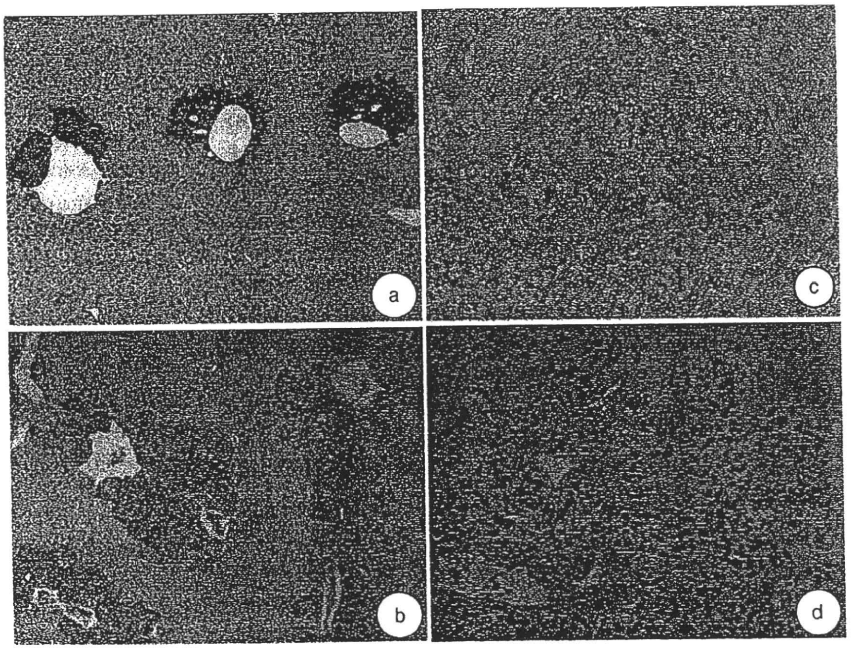

Figure 6 Histological observation of hepatic tissue from graft versus host response (GVHR) mice that were pretreated with the anti-IL-10 mAb. (a) Haematoxylin and eosin (H&E) image of GVHR mice liver that received the control mAb (× 13.5). (b) H&E image in GVHR mice liver that received the anti-IL-10 mAb (× 13.5). (c) Immunohistochemical (IHC) image for IL-10Rβ in GVHR mice that received the anti-IL-10 mAb (× 50). (d) IHC image for Foxp3 in GVHR mice that received the anti-IL-10 mAb (× 50).

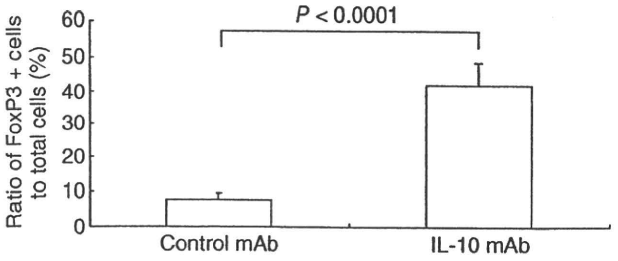

Figure 7 The ratio of positive cells with FoxP3 to the total hepatic infiltrated Inflammatory cells in the anti-IL-10 vs. control IgG mAb-injected mice after 2 weeks. Data are shown as the mean ± SD, and statistically analyzed by unpaired Student's *t*-test. mAB, monoclonal antibody.

the response time for down-regulation by the Tr1 cells after its differentiation in a peripheral site, i.e. in the infiltration site of hepatic tissue, by interaction with $CD4^+CD25^+$Treg cells. In our previous study, the expression of IFN-γ mRNA was elevated as early as 3 days after the spleen T cell injection. By contrast, the expression of the IL-10 mRNA was delayed by 2 weeks when the hepatic inflammation was at its maximum.[2] In the present study, the later expression of IL-10 mRNA after 2 weeks suggest that the recovery step of hepatic inflammation had already begun through the activation of Tr1 cells as a result of the enhanced IL-10 production.

$CD4^+CD25^+$Treg cells have been suggested to control their regulatory function by enhancing the differentiation of the Tr1 cells.[10] Dieckmann *et al.* have shown that the induction of the Tr1 cells *in vitro* by the $CD4^+CD25^+$Treg cells was mediated by cell-cell contact using human $CD4^+CD25^+$Treg cells or by the action of the $CD4^+CD25^+$Treg cells on antigen-presenting cells.[32] Based on the previous findings, the increased expression of Foxp3 in the anti-IL-10mAb injected GVHR mice could be the result of a compensatory or feedback mechanism and the inhibition of the Tr1 cells by anti-IL-10 mAb. Therefore, the findings of the present study lead us to the hypothesis that the Tr1 cells, but not the $CD4^+CD25^+$Treg cells, might directly down-regulate the immunologic response against the hepatic inflammation in the GVHR mice, and however, the $CD4^+CD25^+$Treg cells should be needed to differentiate the the Tr1 cells at the inflammatory sites.

In our previous study, the aggravation of the hepatic inflammatory response in the GVHR mouse model was also induced by concanavalin A (ConA),[4] similarly to the observed effect of anti-IL-10 mAb administration.[5] It has been reported that ConA suppressed the activation and/or proliferation of the $CD4^+CD25^+$Treg cells in the thymus and tonsil.[35,36] These data imply that the pathology of the GVHR model might be aggravated by suppression of either $CD4^+CD25^+$Treg cells or Tr1 cells. In other words, both $CD4^+CD25^+$Treg and Tr1 cells could be necessary for immune tolerance in the GVHR model. However, this hypothesis will need the further confirmation and investigation in the ConA-injected GVHR model.

The NKT cells are $CD4^+$ T cells that express the specific surface marker (CD161) of natural killer cells, and play the role of regulation in immunologic reaction by producing of IL-4 and IFN-γ.[20] Many studies have reported that NKT cells were selectively decreased in model mice and in patients with immune diseases.[37–39] In the present study, although many $CD161^+$ cells were detected in the hepatic inflammatory regions, the cells significantly decreased at G4 and G8 after the transient increase at G2. Furthermore, most of the $CD161^+$ cells did not co-express $CD4^+$ in the fluorescence IHC observation suggesting that the specifically CD161 positive cells are the natural killer cells. In addition, it has been reported that the positive selection in development of NKT cells requires the MHC class I-like molecule, CD1d.[20] On the other hand, the GVHR in the present study was caused by the differences in MHC class II.[7] Therefore, in the GVHR mice, the NKT cells might not be related with the recovery of immunologic response.

In conclusion, the findings of the present study support, at least partially, the expression and activity of the Treg cells as key factors in the induction of immune tolerance in GVHR liver diseases.

ACKNOWLEDGEMENT

A PART OF this study was presented at The 19th The Meeting of Liver and Immunology, The 5th Japan Society of Hepatology Single Topic Conference, The 42nd Annual meeting of Japan Society of Hepatology, and The 107th Annual Meeting of the American Association for the Study of Liver Diseases and the Digestive Disease Week.

The authors also thank the Laboratory Animal Resource Center at the University of Tsukuba for their assistance with the breeding of the experimental animals.

T. Miyazaki and M. Doy contributed equally to this work.

REFERENCES

1 Saitoh T, Fujiwara M, Asakura H. L3t4+ t cells induce hepatic lesions resembling primary biliary cirrhosis in mice

with graft-versus-host reactions due to major histocompatibility complex class II disparity. *Clin Immunol Immunopathol* 1991; 59: 449–61.
2 Itoh S, Matsuzaki Y, Kimura T *et al.* Cytokine profile of liver-infiltrating CD4+ T cells separated from murine primary biliary cirrhosis-like hepatic lesions induced by graft-versus-host reaction. *J Gastroenterol Hepatol* 2000; 15: 443–51.
3 Itoh S, Matsuzaki Y, Kimura T *et al.* Suppression of hepatic lesions in a murine graft-versus-host reaction by antibodies against adhesion molecules. *J Hepatol* 2000; 32: 587–95.
4 Unno R, Matsuzaki Y, Itoh S, Doy M, Shoda J, Tanaka N. Novel murine autoimmune-mediated liver disease model induced by graft-versus-host reaction and concanavalin A. *J Gastroenterol Hepatol* 2001; 16: 1149–57.
5 Unno R, Matsuzaki Y, Itoh S, Doy M, Shoda J, Tanaka N. Progression of autoimmune-mediated hepatic lesions in a murine graft-versus-host reaction by neutralizing IL-10. *Hepatol Res* 2003; 26: 354–61.
6 Van der Veen F, Rolink AG, Gleichmann E. Diseases caused by reactions of T lymphocytes to incompatible structures of the major histocompatibility complex. IV. Autoantibodies to nuclear antigens. *Clin Exp Immunol* 1981; 46: 589–96.
7 Ikarashi Y, Matsumoto Y, Omata S, Fujiwara M. Recipient-derived T cells participate in autoimmune-like hepatic lesions induced by graft-versus-host reaction. *Autoimmunity* 1995; 20: 121–7.
8 Toubi E Targeting T regulatory cells in autoimmune diseases. *Isr Med Assoc J* 2008; 10: 73–6.
9 Toubi E. The Role of CD4+CD25+ T Regulatory Cells in Autoimmune Diseases. *Clin Rev Allergy Immunol* 2008; 34: 338–44.
10 Veldman C, Nagel A, Hertl M Type I regulatory T cells in autoimmunity and inflammatory diseases. *Int Arch Allergy Immunol* 2006; 140: 174–83.
11 Sakaguchi S. Naturally arising Foxp3-expressing CD25+CD4+ regulatory T cells in immunological tolerance to self and non-self. *Nat Immunol* 2005; 6: 345–52.
12 Thompson C, Powrie F. Regulatory T cells. *Curr Opin Pharmacol* 2004; 4: 408–14.
13 Jiang H, Chess L. An integrated view of suppressor T cell subsets in immunoregulation. *J Clin Invest* 2004; 114: 1198–208.
14 Saitoh T, Ikarashi Y, Ito S, Watanabe H, Fujiwara M, Asakura H. Depletion of CD8+ cells exacerbates organ-specific autoimmune diseases induced by CD4+ T cells in semiallogeneic hosts with MHC class II disparity. *J Immunol* 1990; 145: 3268–75.
15 Hori S, Nomura T, Sakaguchi S. Control of regulatory T cell development by the transcription factor Foxp3. *Science* 2003; 299: 1057–61.
16 Khattri R, Cox T, Yasayko SA, Ramsdell F. An essential role for Scurfin in CD4+CD25+ T regulatory cells. *Nat Immunol* 2003; 4: 337–42.
17 Fontenot JD, Gavin MA, Rudensky AY. Foxp3 programs the development and function of CD4+CD25+ regulatory T cells. *Nat Immunol* 2003; 4: 330–6.
18 Powrie F, Maloy KJ. Immunology regulating the regulators. *Science* 2003; 299: 1030–1.
19 Jordan MS, Boesteanu A, Reed AJ *et al.* Thymic selection of CD4+CD25+ regulatory T cells induced by an agonist self-peptide. *Nat Immunol* 2001; 2: 301–6.
20 Seino KI, Fukao K, Muramoto K *et al.* Requirement for natural killer T (NKT) cells in the induction of allograft tolerance. *Proc Natl Acad Sci USA* 2001; 98: 2577–81.
21 Arai T, Hiromatsu K, Kobayashi N *et al.* IL-10 is involved in the protective effect of dibutyryl cyclic adenosine monophosphate on endotoxin-induced inflammatory liver injury. *J Immunol* 1995; 155: 5743–9.
22 Louis H, Le Moine O, Peny MO *et al.* Hepatoprotective role of interleukin 10 in galactosamine/lipopolysaccharide mouse liver injury. *Gastroenterology* 1997; 112: 935–42.
23 Louis H, Le Moine O, Peny MO *et al.* Production and role of interleukin-10 in concanavalin A-induced hepatitis in mice. *Hepatology* 1997; 25: 1382–9.
24 Louis H, Van Laethem JL, Wu W *et al.* Interleukin-10 controls neutrophilic infiltration, hepatocyte proliferation, and liver fibrosis induced by carbon tetrachloride in mice. *Hepatology* 1998; 28: 1607–15.
25 Thompson K, Maltby J, Fallowfield J, McAulay M, Millward-Sadler H, Sheron N. Interleukin-10 expression and function in experimental murine liver inflammation and fibrosis. *Hepatology* 1998; 28: 1597–606.
26 Nagaki M, Tanaka M, Sugiyama A, Ohnishi H, Moriwaki H. Interleukin-10 inhibits hepatic injury and tumor necrosis factor-alpha and interferon-gamma mRNA expression induced by staphylococcal enterotoxin B or lipopolysaccharide in galactosamine-sensitized mice. *J Hepatol* 1999; 31: 815–24.
27 Yoshidome H, Kato A, Edwards MJ, Lentsch AB. Interleukin-10 suppresses hepatic ischemia/reperfusion injury in mice: implications of a central role for nuclear factor kappaB. *Hepatology* 1999; 30: 203–8.
28 Nelson DR, Lauwers GY, Lau JY, Davis GL. Interleukin 10 treatment reduces fibrosis in patients with chronic hepatitis C: a pilot trial of interferon nonresponders. *Gastroenterology* 2000; 118: 655–60.
29 Nelson DR, Tu Z, Soldevila-Pico C *et al.* Long-term interleukin 10 therapy in chronic hepatitis C patients has a proviral and anti-inflammatory effect. *Hepatology* 2003; 38: 859–68.
30 Groux H, O'Garra A, Bigler M *et al.* A CD4+ T-cell subset inhibits antigen-specific T-cell responses and prevents colitis. *Nature* 1997; 389: 737–42.
31 Roncarolo MG, Bacchetta R, Bordignon C, Narula S, Levings MK. Type 1 T regulatory cells. *Immunol Rev* 2001; 182: 68–79.
32 Dieckmann D, Bruett CH, Ploettner H, Lutz MB, Schuler G. Human CD4(+)CD25(+) regulatory, contact-dependent

T cells induce interleukin 10-producing, contact-independent type 1-like regulatory T cells. *J Exp Med* 2002; 196: 247–53.

33 Jonuleit H, Schmitt E, Kakirman H, Stassen M, Knop J, Enk AH. Infectious tolerance: human CD25(+) regulatory T cells convey suppressor activity to conventional CD4(+) T helper cells. *J Exp Med* 2002; 196: 255–60.

34 Foussat A, Cottrez F, Brun V, Fournier N, Breittmayer JP, Groux H. A comparative study between T regulatory type 1 and CD4+CD25+ T cells in the control of inflammation. *J Immunol* 2003; 171: 5018–26.

35 Simark-Mattsson C, Dahlgren U, Roos K. CD4+CD25+ T lymphocytes in human tonsils suppress the proliferation of CD4+CD25– tonsil cells. *Scand J Immunol* 2002; 55: 606–11.

36 Takahashi T, Kuniyasu Y, Toda M *et al.* Immunologic self-tolerance maintained by CD25+CD4+ naturally anergic and suppressive T cells: induction of autoimmune disease by breaking their anergic/suppressive state. *Int Immunol* 1998; 10: 1969–80.

37 Mieza MA, Itoh T, Cui JQ *et al.* Selective reduction of V alpha 14+ NK T cells associated with disease development in autoimmune-prone mice. *J Immunol* 1996; 156: 4035–40.

38 Wilson MT, Van Kaer L. Natural killer T cells as targets for therapeutic intervention in autoimmune diseases. *Curr Pharm Des* 2003; 9: 201–20.

39 Kojo S, Adachi Y, Keino H, Taniguchi M, Sumida T. Dysfunction of T cell receptor AV24AJ18+, BV11+ double-negative regulatory natural killer T cells in autoimmune diseases. *Arthritis Rheum* 2001; 44: 1127–38.

Chapter 30
The Protective Effect of Taurine Against Hepatic Damage in a Model of Liver Disease and Hepatic Stellate Cells

Teruo Miyazaki, Bernard Bouscarel, Tadashi Ikegami, Akira Honda, and Yasushi Matsuzaki

Abstract Taurine plays a protective role against free radicals and toxins in various cells and tissues. However, the effect of taurine on hepatic injury and fibrosis developed by activated hepatic stellate cells (HSC) and myofibroblast-like cells is not fully understood. We investigated the effects of taurine on the hepatic fibrogenesis and damage in rats and isolated HSC. Rats were divided into a normal and two CCl_4-induced liver damage (LD) groups, one untreated and the other maintained for 5 weeks on a 2% taurine diet. The HSC isolated from a normal rat were cultured either for a day only or for an additional 3–6 days with ~50 mM taurine. LD rats maintained on the taurine diet were resistant to CCl_4-induced loss of taurine from the liver. The liver of the LD rats were also protected against histological damage, fibrosis, significant reductions in oxidative stress markers (LPO and 8-OHdG) and hepatic fibrogenic factors (TGF−β_1 mRNA, hydroxyproline, α-SMA). Proliferation, oxidative stress, and fibrogenesis were significantly inhibited in HSC by treatment with taurine. Thus, supplementation with taurine should be considered as a therapeutic approach to lessen the severity of oxidative stress-induced liver injury and hepatic fibrosis.

Abbreviations *HSC*, hepatic stellate cells; *CCl_4*, carbon tetrachloride, *LPO*, lipid hydroperoxide; *TGF−β_1*, transforming growth factor−β_1; *α-SMA*, α-smooth muscle actin protein

T. Miyazaki (✉)
The George Washington University, District of Columbia, USA

J. Azuma et al. (eds.), *Taurine 7*, Advances in Experimental Medicine and Biology 643,
DOI 10.1007/978-0-387-75681-3_30, © Springer Science+Business Media, LLC 2009

30.1 Introduction

Taurine, 2-amino ethylsulfonic acid, is the most abundant amino acid in mammalian tissues, including heart (Awapara 1956), skeletal muscle (Jacobsen and Swimth 1968), nerve, brain, and liver (Jacobsen and Swimth 1968; Huxtable 1980). The plasma and intracellular concentration of taurine are considerably higher than those of other amino acids; plasma: 200~250μM), heart: 25~30mM (Timbrell et al.1995), lung: 11~27mM (Timbrell et al. 1995), neutrophils: 50~100mM (Fukuda et al. 1982; Green 1991), retina: 50~ 70mM (Sturman 1993). The high intracellular levels of taurine are maintained by active uptake and endogenous synthesis ,mainly in the liver where taurine is an endproduct of sulfur amino acid catabolism (Hosokawa et al. 1990; Kaisaki et al. 1995; Reymond et al. 1996; Tappaz et al. 1999). The biosynthesis of taurine in the liver is limited, particularly in the case of liver disease, where the biosynthetic ability might be reduced. Therefore, exogenous uptake via the diet is largely responsible for maintaining the high intracellular concentration of taurine that account for its many physiological and pharmacological roles, including cellular plasma membrane stabilization (Pasantes et al. 1985), osmoregulation (Nieminen et al. 1988), neuromodulation and neurotransmission (Davison and Kaczmarec 1971; Kuriyama 1980; Kanner and Nurit 1994), anti-oxidation (Nakashima et al. 1990; Waterfield et al. 1993a, b; Timbrell et al. 1995), detoxification (Huxtable 1992) and conjugation to bile acids in the liver (Sjovall 1959; Danielsson 1963).

We have demonstrated the effects of taurine on oxidative stress induced by exercise and/or by hepatotoxin in rats. In exercised rats, oral taurine administration reduced oxidative stress (lipid peroxidation, oxidized glutathione) and diminished the decrease in taurine content of skeletal muscle (Miyazaki et al. 2004a). Hepatic taurine concentration was significantly decreased in liver disease mediated by a free radical inducer CCl_4 (Miyazaki et al. 2004b). Previous studies have shown that taurine treatment inhibits hepatic damage induced by CCl_4-mediated oxidative stress (Vohra and Hui 2001; Dinçcer et al. 2002) and thioacetamide-mediated toxicity (Balkan et al. 2001). Indeed, the anti-oxidant activity of taurine has been reported in chick heart (Azuma et al. 1987), hamster lung (Wang et al. 1991; Gordon et al. 1992), and the rat central nervous system (Vohra and Hui 2001), as well as in human lymphoblastoid cells (Pasantes et al. 1984), neutrophils (Wright et al. 1985), and blood cells in culture (Koyama et al. 1992). Therefore, these results show that taurine serves as an anti-oxidant to prevent liver disease.

Oxidative stress and cytokine tranforming growth factor-beta$_1$ (TGF$-\beta_1$) participate closely (Li and Friedman 1999). TGF$-\beta_1$ is mainly released from inflammatory cells, most likely Kupffer cells and neutrophils. It is widely accepted that TGF$-\beta_1$ activates and transforms hepatic stellate cells (HSC; Ito cells, lipocytes, vitamin A-storing cells) into myofibroblast-like cells. The transformed HSC secrete the amino acid, hydroxyproline, which is abundant in collagen-structured and extracellular matrix (ECM) fibrotic tissue. In turn, the HSC transformation induces the augmentation of ECM synthesis (Schafer et al. 1987; Nakatsukasa et al. 1990; Gressner 1996). Transformed HSC characteristically express alpha-smooth muscle

actin (α-SMA) (Enzan et al. 1994). Increased ECM synthesis leads to the progression of fibrosis. Therefore, the inhibition of hepatic damage potentially diminishes both inflammatory cell infiltration (*i.e.* Kupffer cells and neutrophils) and platelet aggregation. Consequently, the secretion of TGF$-\beta_1$ by those inflammatory cells should be reduced, the activation and transformation of myofibroblasts should be decreased and hepatic fibrosis/cirrhosis should diminish (Friedman 1993).

In a previous study, Dinçcer et al. (2002) observed that acute taurine treatment reduced the degree of CCl_4-mediated lipid peroxidation and liver necrosis. However, there is little information on the effect of taurine on chronic hepatic damage and oxidative stress mediated by repetitive administration of CCl_4. Furthermore, the effect of taurine on the activation of HSC remains unclear. Therefore, in the present study, we proposed to examine the effects of taurine on hepatic fibrosis and oxidative damage in a hepatic damage rat model induced by chronic CCl_4 administration and on fibrogenesis and oxidative stress in isolated rat HSC.

30.2 Materials and Methods

30.2.1 Animal Model Experiment

30.2.1.1 Hepatic Disease Rat Model

Male 6-week old rats (Sprague-Dawley; Japan SLC, Shizuoka, Japan) were divided randomly into 3 groups: normal ($N = 8$), liver disease (LD: $N = 18$), and LD treated with taurine (LDT: $N = 18$). The rats in the LDT group were given 2% taurine mixed with standard diet. After 1 week, the rats in the LD and LDT groups were subcutaneously injected 50% CCl_4-olive oil solution as 1 mL/kg body weight twice a week for 5 weeks. As in other studies, they also received 0.05% phenobarbital dissolved in the drinking water (Matsuzaki et al. 2002b; Miyazaki et al. 2003a, b; Miyazaki et al.2004b; Miyazaki et al. 2005; Zhang et al. 2006). Blood and liver were collected from the anesthetized animals. Taurine content was measured by amino acid analysis (Matsuzaki et al. 2002a, 2002b). All rats were kept at 21–25°C under 12-hour dark/light cycles, and received humane care in accordance with *The Guidelines of the University of Tsukuba for the Care of Laboratory Animals.*

30.2.1.2 Fibrosis Analysis

For histological analysis, the liver tissue was embedded on paraffin for Hematoxin & Eosin (HE) and silver staining, and immunohistrochemical (IHC) staining for $\alpha - SMA$. Hepatic fibrosis was quantified from positive silver staining as described in a previous study (Ludwig 1993).

Hepatic hydroxyproline content was used as a measure of fibrosis. Homogenized liver was incubated with 6N HCl at 105°C for 18 hours and centrifuged to get bottom's layer. After drying the pellet, the sample was incubated with chloramine-T

solution at 50°C for 90 min, and the hepatic hydroxyproline concentration was determined by measuring the absorbance at 540 nm by a 96-well plate reader.

TGF–β_1 mRNA content in the liver samples was quantified by real-time PCR. After reverse-transcription of RNA, hepatic TGF–β_1 mRNA content was detected using TaqMan® Universal PCR Master Mix (Perkin Elmer) and an Automated Sequence Detection System (Perkin Elmer). The temperature profile and the sequence of primers and probes for TGF–β_1 and β-actin (internal standard) are as follows: at 50°C for 2 min, at 95°C for 10 min, 40 cycles of at 95°C for 15 sec and at 60°C for 1 min, TGF–β_1 probe; 5'-AGT GGC TGA ACC AAG GAG ACG GAA TAC-3', TGF–β_1 sense primer; 5'-CGC CTG CAG AGA TTC AAG TCA A-3', TGF–β_1 anti-sense primer; 5'-GTC GGT TCA TGT CAT GGA TGG T-3', β-actin probe; 5'-TTT GAC ACC TTC AAC ACC CCA GCC A-3', β-actin sense primer; 5'-CGT GAA AAG ATG ACC CAG ATC A-3', β-actin anti-sense primer; 5'-ACA CAG CCT GGA TGG CTA CGT A-3'. The 5' and 3' terminals in both probes were FAM and TAMRA labeled, respectively. The β-actin probe was designed and provided by Nippon Flour Mills Co., Ltd. (Tokyo, Japan).

The expression of $\alpha - SMA$ protein was determined by Western blotting of homogenized liver.

30.2.1.3 Oxidative Stress Markers

The concentration of lipid hydroperoxide (LPO) and 8-hydroxy-2'-deoxyguanosine (8-OHdG) in serum and liver were used to assess lipid peroxidation and oxidative DNA damage, respectively. The LPO concentration was measured as hydroperoxides utilizing a redox reaction with ferrous ions (Mihaljevic et al. 1996) as described in the LPO assay kit (Cayman chemical company, Ann Arbor, MI). The 8-OHdG concentration was determined using the ELISA detection kit (8-OHdG Check; Japan Institute for the Control of Aging, Shizuoka, Japan).

30.2.2 Hepatic Satellite Cells Experiment

30.2.2.1 Isolation and Culture of HSC

HSC were isolated from normal Sprague-Dawley rat (Japan SLC) by the two-step collagenase perfusion method as described in our previous study (Zhang et al. 2006). Isolated HSC were plated on a 96-well plate at 1×10^4 cells/well and in 35mm plastic culture dishes at 5×10^5 cells/dish and incubated with DMEM containing 10% fetal bovine serum and 100 U/mL penicillin/streptomycin. HSC were cultured at 37°C in a humidified atmosphere of $5\% CO_2$. Activation of HSC was preliminary confirmed after $3 \sim 7$ days of plating, as determined by the loss of vitamin A autofluorescence and the increased expression of $\alpha - SMA$. After 24 hours in culture, the HSC were cultured for an additional 3 days (condition A) and 6 days (condition C) with 0, 25, and 50mM (Tau-0, -25, and -50) taurine, or for an additional 3 days with taurine followed by 3 days of culture without taurine (condition B). The culture

medium was changed every 2 days. The HSC were then harvested. In addition, culture medium before and after the completion of protocols B and C was kept for assays of LPO and hydroxyproline.

30.2.2.2 HSC Proliferation

Cell growth and DNA synthesis were measured by the MTT assay and the $5-bromo-2'$-deoxyuridine (BrdU) cell proliferation assay (Merck Biosciences, Darmstadt, Germany), respectively. Signaling protein expression associated with cell proliferation, such as the total and phosphorylated forms of MAPKs and Akt were determined by Western blotting. The antibodies used were raised against either total or the phosphorylated forms: Thr^{202}/Tyr^{204} p44/42 MAPK, Thr^{180}/Tyr^{182} p38 MARK, Thr^{183}/Tyr^{185} stress activated protein kinase/c-Jun N-terminal kinase (SAPK/JNK) and Ser^{473} Akt, respectively (Cell Signaling Technology, VA).

30.2.2.3 Transforming of HSC, Fibrogenesis, and Oxidative Stress Assays

In the harvested HSC subjected to condition A, the expression levels of $\alpha - SMA$ protein and TGF$-\beta_1$ mRNA was detected by Western blotting and real-time PCR, respectively, as described above. The LPO and hydroxyproline concentrations were determined in the culture medium collected before and after incubation with taurine.

30.2.3 Statistical Analysis

All data are presented as the means $\pm SD$. Significant differences were determined by the unpaired student's t-test, the one-way ANOVA post hoc Fisher's PLSD test or the Mann-Whitney U-test. Statistical significance was set at $p < 0.05$.

30.3 Results

30.3.1 CCl_4-Exposed Rats Treated with Taurine

30.3.1.1 Blood Biochemical Analysis and Taurine Concentration

Serum aspartate aminotransferase (AST) and alanine aminotransferase (ALT) were significantly increased in the LD group compared to that of the normal and LDT group, although ALT levels of the LDT were significantly higher than those of the normal group (Fig. 30.1). Total serum bilirubin content was increased eight-ten-fold in the LD and LDT groups compared to that of the normal, however there was no significant difference between the LD and LDT groups. Furthermore, serum albumin levels in the LD and LDT groups tended to be lower than those of the normal group; there was no significant difference between the LD and LDT groups. Serum taurine concentration of the LD group was unchanged relative to the normal, but levels

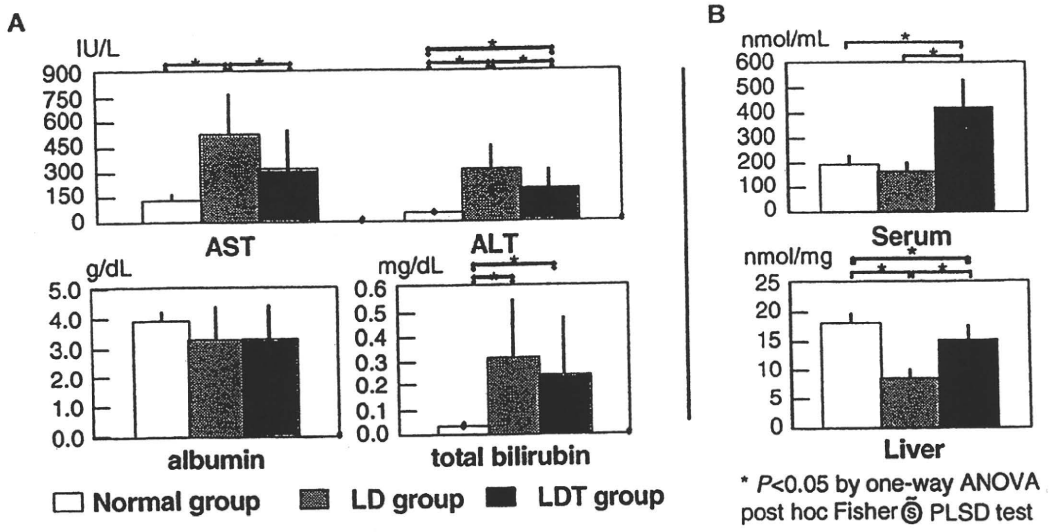

Fig. 30.1 Blood biochemical analyses and taurine concentration in serum and liver of CCl_4-treated rats with or without dietary taurine supplementation. **A**: Serum analysis of liver function, **B**: Taurine concentration in serum and liver. Data represent means ±SD

of the LDT groups were increased more than two-fold compared to those of the normal and LD groups (Fig. 30.1B). On the other hand, hepatic taurine content was significantly decreased in the LD group compared to that of the normal group; oral taurine administration preserved hepatic taurine levels against depletion observed in the LD group.

30.3.1.2 Histological Hepatic Pathology

Based on HE staining, CCl_4-administered rat livers underwent fibrosis, marked fatty degeneration, necrosis, cellular inflammation and infiltration of inflammatory cells including macrophages and lymphocytes. In the LD group, this damage was found throughout the liver and fibrotic infiltrations appeared in both the pericentral and periportal regions, with bridging fibrosis seen (Fig. 30.2). In the LDT group, hepatic necrosis and infiltration of inflammatory cells were inhibited compared to the LD group, particularly in the pericentral region. Similarly, the development of hepatic fibrosis was diminished in the pericentral region, the degree of bridging fibrosis was

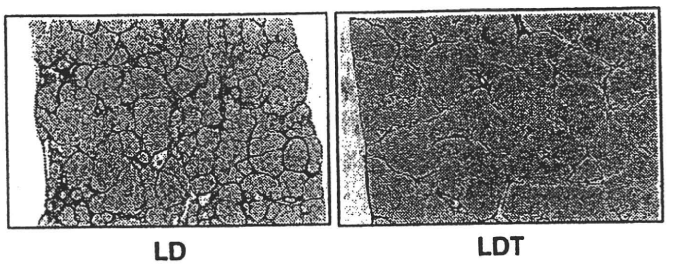

Fig. 30.2 Light micrographs of silver stained liver. Objective was ×5